NEMO 3 — A DOUBLE-BETA DECAY EXPERIMENT WITHOUT NEUTRINO EMISSION*

Danielle Dassie

CEN-Bordeaux-Gradignan, France

and NEMO Collaboration

CEN-Bordeaux-Gradignan, France
CFR-Gif/Yvette, France
IReS-Strasbourg, France
Department of Physics-Jyvaskyla, Finland
FNSPE-Prague, Czech Republic
INEEL-Idaho Falls, USA
ITEP-Moscow, Russia
JINR-Dubna, Russia
LAL-Orsay, France
MHC-South Hadley, USA

(Received December 1, 1998)

The physics goals of double beta decay experiments are reminded. Various experimental aspects of the NEMO experiment are presented and the expected performances of NEMO 3 compared with previous or forthcoming other experiments.

PACS numbers: 23.40.–s, 29.40.Gx

1. Introduction

Oscillations of atmospheric neutrinos observed in the Superkamiokande experiment [1] made the problem of neutrino masses and neutrino mixing enter an era of new actuality. An understanding of the physical origin of the masses will however require further experiments. The neutrinoless double beta decay process $(\beta\beta)_{0\nu}$, plays a privileged role in the investigation of the nature of the neutrino and its existence would be a probe for physics beyond the standard model of electro-weak interactions. Neutrinoless double

* Presented at the XXXIII Zakopane School of Physics, Zakopane, Poland, September 1–9, 1998.

beta decay occurs only when the neutrino is of Majorana type with a finite mass. Besides neutrino mass, the potential of double beta decay includes investigation of right-handed W bosons, Majorons, SUSY models ...

The present contribution will report on neutrino studies by measuring double beta decays with the detector NEMO 3. The NEMO (Neutrino Experiment with MOlybdenum) experiment will be able to study $(\beta\beta)_{0\nu}$ decays of nuclei with half-lifes up to 10^{25} years. Using relevant nuclear matrix elements this corresponds to an effective Majorana neutrino mass of the order of 0.1-0.3 eV. The detector is under construction and will be completed by the end of 1999.

2. Double beta decay

Double beta decay is a transition between nuclei with the same mass number and differing by two units in protons. It is potentially observable when single beta decay to the intermediate nucleus is forbidden by energy conservation or large angular momentum differences (Fig 1).

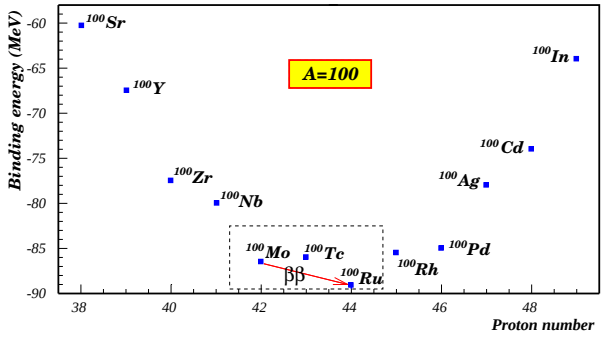


Fig. 1. Binding energy as a function of Z for A=100 isobars.

Double beta decay can occur in several processes:

$$
\begin{aligned}
{}^{A}_{Z}X &\longrightarrow {}^{A}_{Z+2}X + 2e^- + 2\overline{\nu}_e \quad (1)\\
{}^{A}_{Z}X &\longrightarrow {}^{A}_{Z+2}X + 2e^- \quad (2)\\
{}^{A}_{Z}X &\longrightarrow {}^{A}_{Z+2}X + 2e^- + \chi \quad (3)
\end{aligned}
$$

Although rare, decay (1) is allowed as a second effect in the standard model of the electro-weak interaction. It has indeed been firmly established by experiments. Decay channels (2) and (3) are more interesting since lepton number conservation is violated and as a consequence they test physics beyond the standard model. In the $(\beta\beta)_{0\nu}$ decay, the virtual neutrino must be emitted in one vertex and absorbed in the other one. Since in the standard

theory the emitted particle is a right-handed antineutrino and the absorbed one a left-handed neutrino, the process requires that the exchanged neutrino is a Majorana particle $\nu = \overline{\nu}$ and that both neutrinos have a common helicity component. The helicity matching restriction can be satisfied either if the neutrinos have a nonvanishing mass and therefore a "wrong" helicity component proportional to m_ν/E_ν or if there is a right-handed-current weak interaction, but a non vanishing mass is required in any case [2].

The effective Majorana neutrino mass to which $(\beta\beta)_{0\nu}$ experiments are sensitive is generally written in terms of the electron neutrino mixing matrix $U_{e,j}$ as:

$$\langle m_\nu \rangle = \sum_j \epsilon_j m_j U_{e,j}^2 \,,$$

where m_j are the mass eigenstates and ϵ_j phase factors.

The transition rate for $(\beta\beta)_{0\nu}$ events with a Majorana neutrino mass $\langle m_\nu \rangle$ and neglecting the right-handed-current terms is given as :

$$[T_{1/2}^{0\nu}]^{-1} = G^{0\nu} |M^{0\nu}|^2 \langle m_\nu \rangle^2 \,,$$

where $G^{0\nu}$ is a calculable phase space factor, $|M^{0\nu}|$ is the nuclear matrix element.

Important to note that the transition rate strongly depends on the nuclear matrix element and various models can lead to different values of $T_{1/2}^{0\nu}$.

Experimentally the three decay modes $(\beta\beta)_{2\nu}$, $(\beta\beta)_{0\nu}$ and $(\beta\beta)_{0\nu\chi}$ are studied by measuring the sum energy of the two electrons. Fig. 2 shows schematically the corresponding spectra. In the case of the neutrinoless mode a sharp discrete line at $E=Q_{\beta\beta}$ is expected. For the two-neutrino mode as well as for the Majoron accompanied mode a continuous spectrum will be observed.

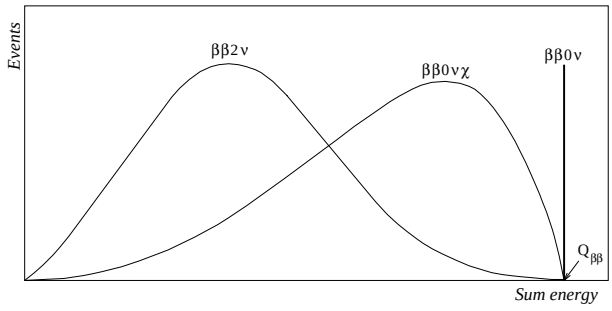


Fig. 2. Possible double beta signals.

3. The NEMO experiment

The tiny probability associated with a double beta decay event represents a severe experimental challenge. Indeed, a process with a half-life of the order of 10^{25} years must be detected in the presence of inevitable traces of radioisotopes with similar energy release, but having decay rates larger by more than ten orders of magnitude. These impurities, particularly those from uranium and thorium decay chains or those from cosmic origin are a serious source of background.

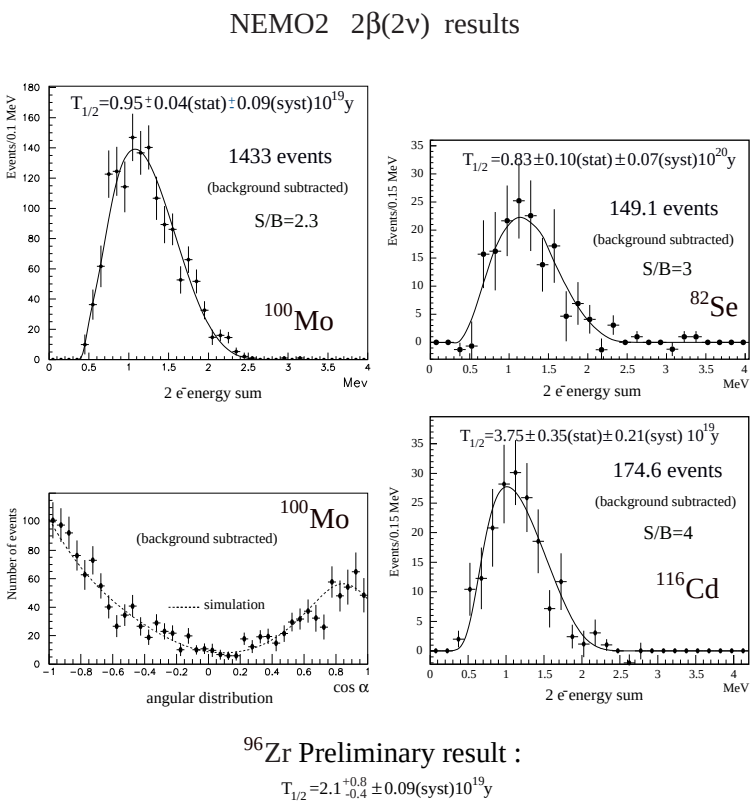


Fig. 3.

In 1989 the NEMO collaboration started an R & D program. Two prototype detectors NEMO 1 and NEMO 2 were constructed using reliable experimental techniques which allowed to fully characterize the decay and the backgrounds. The prototype detector NEMO 1 [3] was constructed to test the tracking of electrons. NEMO 2 [4] was designed to identify and measure the different backgrounds. Unlike most beta decay experiments this prototype had the capacity to study "source" foils of different materials

and NEMO 2 measured the allowed process $(\beta\beta)_{2\nu}$ of three isotopes ^{100}Mo, ^{116}Cd and ^{82}Se (Fig. 3) [5–7]. These emitters fulfill two conditions : high isotopic abundance to make possible large quantities of enriched materials and high $Q_{\beta\beta}$ to increase the phase space factor and to push the expected $(\beta\beta)_{0\nu}$ signal above the natural radioactive background. The prototype NEMO 2 was operating during 6 years in the Frejus Underground Laboratory where the muon rate is decreased by a factor 10^6.

3.1. NEMO 3 design

The detector is cylindrical and divided into 20 equal sectors (Fig. 4). It consists of a tracking volume filled with helium gas, a thin (50 μm) source foil divides the tracking volume into two concentric cylinders. The surfaces of these cylinders are covered by calorimeters constructed with 1940 large blocks of polystyrene scintillators coupled to low radioactivity photomultiplier tubes. Two types of PMTs are used (3" and 5") depending on the size of the blocks. The tracking system consists of 6180 vertical open octogonal Geiger cells.

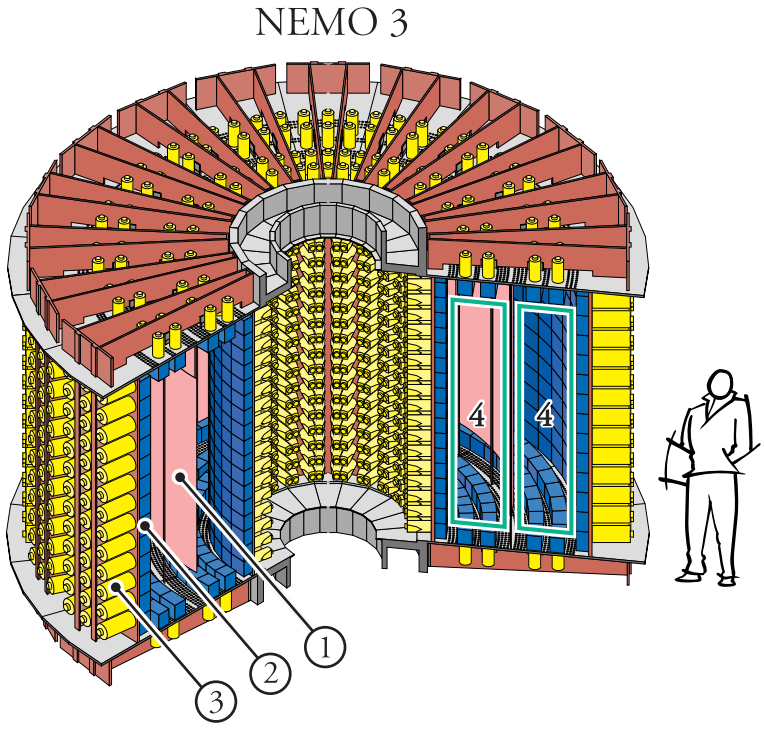


Fig. 4. (1) — cylindrical source foil; (2) — scintillator blocks; (3) — photomultiplier tubes; (4) — tracking volume of drift cells.

NEMO 3 [8] will be able to accomodate up to 10 kg of various double beta decay candidates. To date, attention has been focused on 10 kg of enriched Molybdenum (97% ^{100}Mo). Also available, is one kilogram of each isotope ^{82}Se, ^{116}Cd and ^{130}Te. A solenoid producing a field up to 50 Gauss will surround the detector to reject pair effect events coming from external γ ray background. Finally, external shielding in the form of 20 cm of low activity iron will reduce the γ ray flux and thermal neutrons.

3.2. Background

Of primary importance to all $\beta\beta$ decay experiments is the reduction of radioactivity arising from the uranium and thorium decay chains, in particular the decay of ^{214}Bi and ^{208}Tl which can generate background events which mimic $\beta\beta$ signal. Careful attention is also paid to the ubiquitous potassium.

Events looking like double beta events and not rejected by time of flight measurements can be created either by gamma rays interacting in the foil or by contamination in the foil. Gamma rays interacting in the foil can simulate a good event by a two step process (for example double Compton effect or Compton+Möller effect) where two electrons are emitted and photons escape. Beta emitter contamination in the foil can also mimic double beta events when for example a beta particle is emitted simultaneously with another electron (for instance converted γ ray or Möller scattering). All the materials which have gone into the construction of the detector have been examined with HP Ge detectors at the Fréjus Underground Laboratory or at the C.E.N.B.G. laboratory in Bordeaux. This exhaustive examination of samples caused the rejection of numerous glues, plastics, and metals. The activity in the mechanical pieces which frame the detector are required to be less than 1 Bq/kg. As expected, the radioactive contamination in the experiment is dominated by low radioactivity glass in the PMTs. The total activity of all of the 0.6 tons of PMTs is 800 Bq of ^{40}K, 300 Bq of ^{214}Bi and 18 Bq of ^{208}Tl. These levels are three orders of magnitude below standard PMT levels. There are two sources of plastic scintillators, both with very low levels of radiation. Specifically, from Dubna there are 4 tons with less than 10 Bq of ^{40}K, approximately 5.2 Bq of ^{214}Bi and less than 2 Bq of ^{208}Tl. The one ton of Kharkov scintillators has less than 10 Bq of ^{40}K, 0.7 Bq of ^{214}Bi and 0.3 Bq of ^{208}Tl. The experimental hall for NEMO 3 is in the Fréjus Underground Laboratory at a depth of 4800 meters of water equivalent. This reduces the cosmic ray muon flux to 4 m^{-2} per day. Vigorous flushing of the air in the hall reduces the radon levels to 10-20 Bq/m^3. The presence of ^{214}Bi decays in the detector from this level of contamination is below that introduced by the PMTs, thereby reducing concerns about additional reductions. Photons of natural radioactivity (<2.6 MeV) are troublesome

when interacting with the foil for the $(\beta\beta)_{2\nu}$ and $(\beta\beta)_{0\nu\chi}$ modes. It is not the case for the $(\beta\beta)_{0\nu}$ process and for the chosen $\beta\beta$ emitters, where the energy region of interest $Q_{\beta\beta}$ is above the natural radioactivity limit. In this case the main origin of high energy gamma rays ($\geq$3 MeV) is therefore due to neutron capture inside the detector. Thermal and fast neutrons in the hall are found to be respectively at levels of 1.6×10^{-6} neutrons/s·cm^2 and 4×10^{-6} neutrons/s·cm^2. The effects of these neutrons on the earlier experiment NEMO 2 were studied with an Am-Be source and different formats and levels of shielding. Recent analyses with the software program MICAP is in good agreement with the current understanding of neutron induced backgrounds. In summary thermal neutrons are stopped in the iron shield while fast neutrons go through and are thermalized in the plastic scintillator blocks. The thermalized neutrons are then captured on the copper walls that support the calorimeter producing γ rays up to 8 MeV. Simulations also generate a spectral line at 2.2 MeV suggesting that capture in the scintillators is also significant. However the rates of high energy γ rays interacting with the source foil and producing two electron events or pair creation are expected to be negligible. The magnetic field will be used to study the pair production and confirm the prediction of a negligible contribution. If necessary a paraffin shield surrounding the detector can be added.

As previously stated, the second source of background comes from contamination in the foils. In the $Q_{\beta\beta}$ energy region, there is activity from ^{214}Bi and ^{208}Tl. Of course in the same energy region, the tail of the $(\beta\beta)_{2\nu}$ decay distribution will also play a role. The $(\beta\beta)_{2\nu}$ decays ultimately define the upper half-lives for which the $(\beta\beta)_{0\nu}$ decays can be studied. To insure that the $(\beta\beta)_{2\nu}$ process indeed defines this limit, maximum levels of ^{214}Bi and ^{208}Tl were calculated. These limits are given in Table I. For ^{100}Mo it is believed that these limits have been reached, whereas for ^{82}Se with a longer $(\beta\beta)_{2\nu}$ decay half-life, more stringent levels are sought and will require some additional research. Note that the energetic decay of ^{150}Nd ($Q_{\beta\beta} = 3.7$ MeV) removes concerns of contamination by ^{214}Bi ($Q_\beta = 3.3$ MeV), but new techniques to enrich Nd will have to be developed for this to be realized.

TABLE I

NEMO 3 backgrounds and purity criteria in a 400 keV energy window centered around $Q_{\beta\beta}$.

Isotope	Events/year·10kg			mBq/kg	
	^{214}Bi	^{208}Tl	$\beta\beta2\nu$	^{214}Bi	^{208}Tl
^{100}Mo	0.4	0.4	1.1	0.3	0.02
^{82}Se	0.1	0.1	0.1	0.07	0.005
^{150}Nd	none	0.4	1.1	none	0.02

Currently the plan is to have the ^{100}Mo source foils produced by two different processes. The first is a purification by local melting of solid Mo with an electron beam and drawing a monocrystal from the liquid portion. The monocrystal leaves behind the impurities in the slag of the melt. The crystal is then rolled into a foil for use in the detector. The second purification method is chemical in nature and leaves the Mo in a powder form that is then used to produce foils with a binding paste and mylar strips which have been etched with an ion beam.

4. Expected performances of NEMO 3 and comparison with previous and forthcoming experiments.

Currently, the energy resolution for the calorimeter modules associed with the 5" PMTs is 11% at 1 MeV (FWHM), while it is 14.5% for the modules associed with the 3" PMTs. Taking into account the measured energy resolution, Monte Carlo simulations predict a 14% efficiency in the energy window 2.8 to 3.2 MeV (^{100}Mo case). Assuming 10 kg of ^{100}Mo it is expected 2 background events per year in the same energy region. In figure 5 the expected performances of NEMO 3 are reported for 10 kg of three different isotopes ^{100}Mo, ^{82}Se and ^{150}Nd and for 5 years of data acquisition.

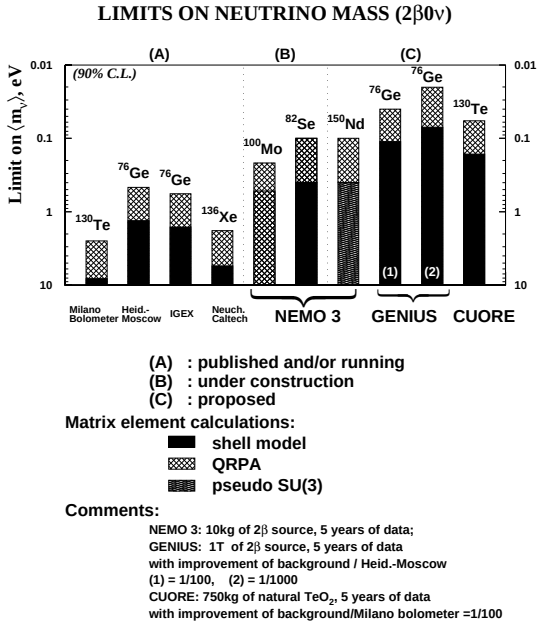


Fig. 5.

The presented effective neutrino mass limits are deduced from three different nuclear matrix element calculations: namely QRPA [9–10], Shell Model [11] and SU(3) [12].

For comparison, other experiments are also reported in figure 5. Part A illustrates the performances of published or running experiments. The best limits today come from the ^{76}Ge experiments, but the traditional argument for high energy resolution is weakened by the larger sensitivity to background events given the lower $Q_{\beta\beta}$ value (2.04 MeV). As shown in Table II, the Heidelderg–Moscow experiment [13–14] reports a significant reduction of the background when using pulse shape discrimination (PSD). The IGEX [15] experiment has reported similar results in the same energy window. Also given in this table are results on ^{136}Xe from the Neuchâtel–Moscow–PSI experiment [16] and on ^{130}Te studied by the Milano group [17]. The latter values are first results of an ongoing research and development programme.

TABLE II

Summary of background and energy resolution for various experiments.

Experiment	Background cts/keV·kg·y	Energy resolution
Heidelberg-Moscow		
no PSD	0.20	3.6 keV at 2 MeV
PSD	0.07	3.6 keV at 2 MeV
IGEX	0.10	3.6 keV at 2 MeV
Neuchâtel-Caltech-PSI	0.018	105 keV at 2.5 MeV
TeO_2 Bolometer	0.48	10 keV at 2.6 MeV
NEMO 3	0.0005	400 keV at 3 MeV

GENIUS (Germanium in Nitrogen Underground Setup) and CUORE (Cryogenic Underground Observatory for Rare Events) proposals are conceptual designs of next generation experiments.

GENIUS's proposed functionality [18] far exceeds that of a double beta decay detector. This ambitious proposal deals with one to ten tons of naked enriched germanium detectors suspended in a liquid nitrogen shield. The background design criteria are 0.04 10^{-3} counts/keV.y.kg which argues an impressive 3.5 orders of magnitude reduction in the background compared to current ^{76}Ge experiments. To be more realistic, predictions with a factor of 100 or even 1000 improvement in the background over the current Heidelberg-Moscow experiment are reported in part C of figure 5 assuming one ton of ^{76}Ge crystals and five years of data taking.

CUORE is the next generation detector under investigation by the Milano group using 750 kg of natural TeO_2 as a bolometer. An improvement of the background by a factor 100 compared to the present experiment has been assumed.

Compared to all other experiments, NEMO 3 shows very promising performances and has furthermore the possibility of using selected $\beta\beta$ emitters with high $Q_{\beta\beta}$ value and with favorable nuclear matrix elements. It is expected that this experiment will bridge the gap between present and far future double beta decay studies using Ge detectors.

5. Status of the construction

Of the 20 sectors required to complete the tracking and calorimeter portions of the detector, 14 will be completed by the end of 1998. We plan to start the experiment early year 2000, operating with 7 kg of ^{100}Mo and 1 kg of ^{82}Se, some sectors filled with foils especially designed to check the background.

REFERENCES

[1] Y. Fukuda *et al.*, *Phys. Rev. Lett.* **81**, 1562 (1998).
[2] M. Doi *et al.*, *Prog. Theor. Phys. Sup.* **83** (1985).
[3] D. Dassié *et al.*, *Nucl. Instrum. Meth.* **A309**, 465 (1991).
[4] R. Arnold *et al.*, *Nucl Instrum. Meth.* **A354**, 338 (1995).
[5] D. Dassié *et al.*, *Phys. Rev.* **D51**, 289 (1995).
[6] R. Arnold *et al.*, *Z.Phys.* **C72**, 239 (1996).
[7] R. Arnold *et al.*, *Nucl. Phys.* **A636**, 209 (1998).
[8] D. Lalanne and C.S. Sutton, Report LAL-Orsay 98-52.
[9] A. Staudt *et al.*, *Europhys. Lett.* **13**, 31 (1990).
[10] T. Tomoda, *Rep. Prog. Phys.* **54**, 53 (1991).
[11] E. Caurier *et al.*, *Phys. Rev. Lett.* **77**, 1954 (1996).
[12] M. Hirsh *et al.*, *Nucl. Phys.* **A582**, 124 (1995).
[13] M. Günther *et al.*, *Phys. Rev.* **D55**, 54 (1997).
[14] L. Baudis *et al.*, *Phys. Lett.* **B407**, 219 (1997).
[15] C.E. Aalseth *et al.*, Proceedings of Neutrino '96, 1997, p. 361.
[16] J.C. Vuilleumier *et al.*, *Phys. Rev.* **D48**, 1009 (1993).
[17] A. Alessandrello *et al.*, *Phys. Lett.* **B335**, 519 (1994).
[18] J. Hellmig *et al.*, *Z. Phys.* **A359**, 351 (1997).